Three Dimensional Finite Element Analysis of Heat Flow in Arc Welding

by

A. K. PATHAK*, and G. L. DATTA**

*Sr Lecturer, Prodn Engg and Mgt Dept, RIT Jamshedpur, 831014

** Professor, Mechanical Engineering Department, IIT Kharagpur, 721302

Presented at The International Welding Conference (IWC'99) on Welding & Allied Technology "Challenges In 21st Century" organised by the IIW in association with CII, 15-17 February 1999, New Delhi

ABSTRACT

In the present paper a three dimensional transient finite element analysis of heat flow in arc welding has been presented. The problem was solved by considering the important factors that influence the heat transfer in arc welding, like, temperature dependent material properties, enthalpy and stirring effect in the molten pool. To reduce the computation time, finer mesh was generated where temperature gradient was too high and gradually mesh size was increased away from the heat source. Variations of temperature along the cross section at two positions of the arc were plotted and compared with the experimental and calculated values available in the literature. Temperature history curve was also plotted and compared with the published results.

INTRODUCTION

Welding is a very old manufacturing process known to mankind. Though it is a very important and popular method of fabrication, it is associated with some problems such as those resulting from heat transfer into the work-piece. In the past, many such problems have been tackled through experimental investigations, requiring collection of extensive data. Cost involved in collection of data is very high and this is also not very convenient for scientific analysis. Fortunately, due to the advent of computer, scientific analysis can now be done much more easily.

In case of arc welding, the electrode and the base metal are heated above their melting points and allowed to cool in atmospheric condition. Due to the temperature differences in the different portions of the heat affected zone and the base materials and different cooling rates, metal transforms to have different micro-structures and develops residual stresses. It has been well established, that micro-structures, residual stresses and other mechanical properties of the weldment depend on the temperature distribution and the cooling rate of the heat affected zone [16,18,4,17].

The study of heat flow in welding has a long history. Rosenthal (1941, 1946) was the first to give the closed analytical solution of classical heat conduction equation [1,2]. Rosenthal made several assumptions to simplify the problem to determine the temperature distribution and cooling rates in welding. Due to these assumptions Rosenthal's analysis is subject to serious error for temperature in or near the fusion and heat affected zones at high temperatures. After Rosenthal, several researchers worked in the same direction to improve the Rosenthal solution.

It is known that the physical properties of materials are temperature dependent. During the welding process, phase change also takes place and heat is dissipated by all the three modes. The distribution of heat flux in the arc is not uniform and can be assumed to be a Gaussian distributed function. Thus the practical welding process is a very complex one to be represented analytically. Hence, many researchers went for numerical methods to get close approximate solutions. In order to

LATEST GENERATION WELDING MACHINES FROM THE PIONEER

SURARC

T-series Fully Thyristor based Rectifier

Move-series CO_2/MIG Welder

SUR IRON has been manufacturing welding machines for more than four decades and is one of the largest manufacturers of arc welding machines in India. Our recent collaboration with **OSAKA DENKI (DAIDEN), JAPAN** reflects our total commitment to our valued customers in serving them with latest products and services.

SURARC PRODUCT RANGE

- AN&AF series Air Cooled AC Welder: 150 – 600 Amps
- XR series D.C. Rectifier Welder: 300 – 600 Amps
- T series Fully Thyristorised D. C. Welder: 350 – 600 Amps
- AFT series A. C. TIG Welder : 300 – 600 Amps.
- GTT series D. C. Thyristorised TIG Welder : 350 – 600 Amps
- ARC star series IGBT Inverters : 160 & 250 Amps
- DWG series diesel engine driven welding generator : 300 – 500 Amps
- Pedestal Type Spot Welder
- Move series fully thyristorised CO_2/MIG 250 & 400 Amps manufactured in collaboration with OSAKA DENKI, Japan
- MECHWELD series automatic submerged ARC Welder : 600, 800 & 1200 Amps
- Welding Column & Boom, Positioners, Rotators & Custom built welding systems.

FIELDKING DWG series Portable Diesel Engine Driven Welding Generator

PANORAMA

SISCO

SUR IRON & STEEL CO. (P) LTD.

15 Convent Road, Calcutta 700014 Phone: 244 8359/1307, 245 4179
Fax: +91(33) 244 1308 Cable: CALSISCO
Mumbai Office : 483 Central Facility, Building - 2, APMC -2,
Sector -19, Vashi, Navi Mumbai 400 705 Phone : (022) 765 8885

avoid the singularity in the heat capacity at the liquid-solid phase transformation, the enthalpy concept was adopted by some researchers [10,11,14]. Convection inside the molten pool was modelled by the enhanced value of thermal conductivity of molten material [5,11]. The stirrer effect in the molten metal was simulated by using a large value of thermal conductivity for temperatures exceeding the melting temperatures [8,12]. Moreover, in the finite element analysis, the accuracy and efficiency of the solution depend strongly on the adaptation scheme that permits mesh refinement only in the required region [15,20].

Most of the researchers have analysed the two dimensional model of heat transfer in welding by considering some of the actual conditions mentioned above. Three dimensional thermal analysis [19] is however very limited. In the present paper a three dimensional problem of welding was solved by incorporating most of the above mentioned concepts and results were compared with the known published results.

List of symbols used

G	=	Rate of heat generation per unit volume per unit time, (W/m^3)
K	=	Thermal conductivity, (W/(m.K))
K_x, K_y, K_z	=	Thermal conductivity in x, y, z directions, (W/(m.K))
Q	=	Arc Power, (W)
S	=	Surface
T	=	Temperature, (^{o}C)
T_∞	=	Temperature of the surrounding, (^{o}C)
V	=	Volume, (m^3)
c	=	Specific heat, (J/(Kg.K))
h	=	Convective heat transfer coefficient, (W/(m^2.K))
l_x, l_y, l_z	=	Direction cosines of outward normal to the boundary
q	=	Heat flux, (W/m^2)
t	=	Time, (s)
x, y, z	=	Coordinates
v	=	Arc travel speed, (m/s)
ρ	=	Density of the base metal, (Kg/m^3)
η	=	Heat efficiency of the arc

Thermal modes

To solve the three dimensional finite element problem, the present authors have made the following assumptions :

- All the thermal properties are considered as functions of temperature. It is assumed that due to thermal expansion, density and element shape are not affected.
- to avoid the sharp change in the heat capacity due to melting, enthalpy of the metal as a function of temperature is considered [9].
- On the boundary, linear Newtonian convective cooling is assumed. No forced convection is considered [7,12,15].
- Since radiation losses are small, they are neglected [20].
- Heat source is assumed to have a Gaussian distribution of heat flux on the surface of the work piece [13,15,18,20].
- Stirrer effect in the molten metal is simulated by using a large value of thermal conductivity for temperatures exceeding the melting temperature [8,12]. The temperature field in molten metal is thus governed by the same equation as is applied to the solid metal [8,14].
- Arc efficiency and melting efficiency reported in literature are properly incorporated to account for other losses.

The governing differential equation for heat conduction in solid is

$$\frac{\partial}{\partial x}\left(K_x\frac{\partial T}{\partial x}\right)+\frac{\partial}{\partial y}\left(K_y\frac{\partial T}{\partial y}\right)+\frac{\partial}{\partial z}\left(K_z\frac{\partial T}{\partial z}\right)+G=\rho c\frac{\partial T}{\partial t} \quad (1)$$

Boundary and initial conditions :
It is pre-assumed that these cover the entire element

$$T = T_\infty \text{ for } t = 0 \quad (2)$$

$$-K_x\frac{\partial T}{\partial x}l_x-K_y\frac{\partial T}{\partial y}l_y-K_z\frac{\partial T}{\partial z}l_z=h(T-T_\infty), \text{on surface S or } t>0 \quad (3)$$

The functional formulation equivalent to Eqn. 1 with its boundary conditions given in Eqns. 2 and 3 is given [6] as

$$\chi=\int_V\frac{1}{2}\left[K_x\left(\frac{\partial T}{\partial x}\right)^2+K_y\left(\frac{\partial T}{\partial y}\right)^2+K_z\left(\frac{\partial T}{\partial z}\right)^2\right.$$

$$\left.-2\left(G-\rho c\frac{\partial T}{\partial t}\right)T\right]dV \quad +\int_S\left[\frac{1}{2}h\,(T-T_\infty)^2\right]dS \quad (4)$$

The final system of equation can be expressed as

$$[C]\frac{\partial\{T\}}{\partial t}+[K]\{T\}+\{F\}=0 \quad (5)$$

Fig. 1 shows the variation of thermal conductivity with temperature [14]. Curve was rounded to avoid sharp variation and enhanced values (8% increment at 1500°C) of thermal conductivity were extrapolated at higher temperatures to compensate for the stirrer effect in the molten zone. Values of enthalpy were calculated from the values of heat capacity reported in reference [14] and plotted in Fig. 2 with suitable adjustment wherever necessary. Temperature dependency of the convective coefficient is shown in Fig. 3.

Transient heat flow analysis due to moving arc

Fig. 4 shows the plates to be welded by arc welding. The heat transfer from the welding arc at any time, on the surface of the weldment, was assumed to be a radially symmetric normal distribution function [3]. Let r be the distance from the weld line in the section at x = 0, and t = 0 (the time at which the centre of the heat source (electrode) passes over this section), the heat flux distribution on the surface of the weldment, is given by :

$$q(r,t)=\frac{3\eta Q}{\pi\bar{r}^2}\,exp\left[-3\left(\frac{r}{\bar{r}}\right)^2\right]exp\left[-3\left(\frac{vt}{\bar{r}}\right)^2\right] \quad (6)$$

where $\bar{r}$ defines the region in which 95 percent of heat flux is deposited.

The transient heat flow analysis was carried out for an average welding speed of 3.33 mm/s and heat input rate of 1680 W. The room temperature was taken equal to 25°C. Assuming arc efficiency equal to 85%, problem was solved with the help of ANSYS 5.0. To improve the accuracy of the result, element size was kept smaller around the heat source where temperature gradient was too high and it was gradually increased away from the heat source. Heat source was moved from one end of the work piece to the other end and temperature distributions were plotted for the various positions. Figs. 5 and 6 show the type of meshing and temperature distribution at 3.603 second respectively. The same at t = 18.018 s and 32.432 s are shown in Figs. 7 to 10. Figs. 11 and 12 are plotted to compare the variation of temperature along the cross section with the experimental and calculated values reported in references [14,20]. Fig. 13 compares the variation of temperature of a point during arc welding with known theoretical and experimental results. It clearly shows that the temperature of the point increases rapidly when arc approaches it and cooling takes place gradually after passing the arc. Cooling rates can also be calculated from the curve.

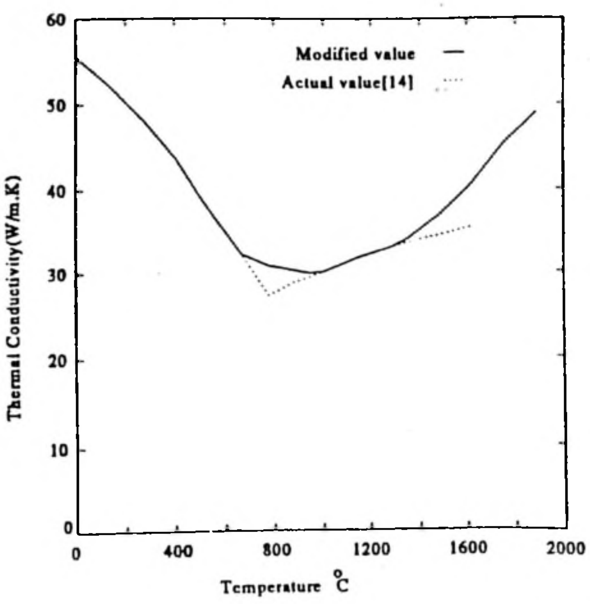

Fig 1 : Thermal Conductivity of mild steel St 37

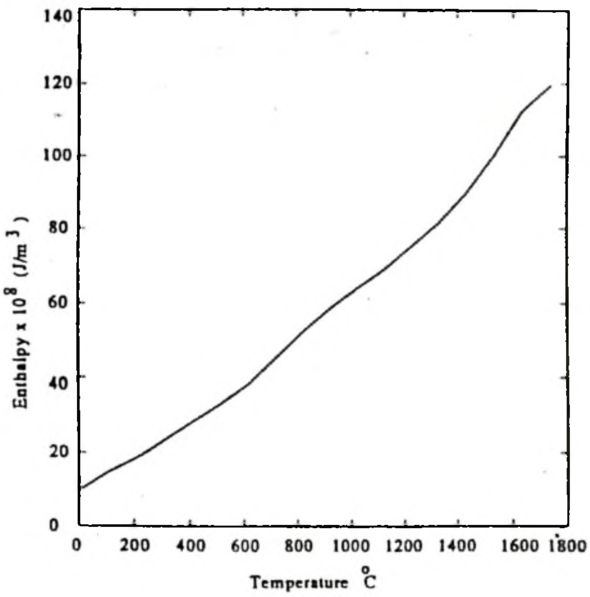

Fig 2 : Enthalpy of mild steel St 37

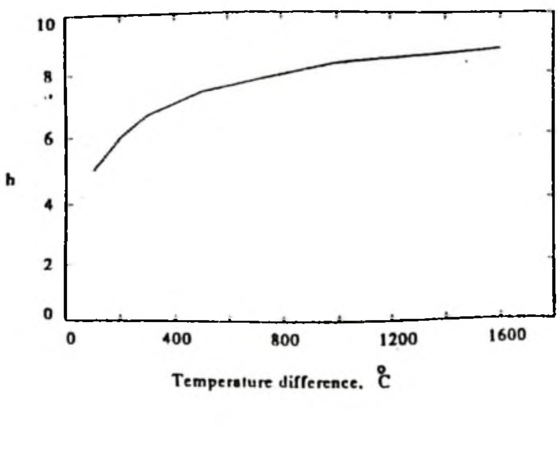

Fig 3 : Convective heat transfer coefficient [14]

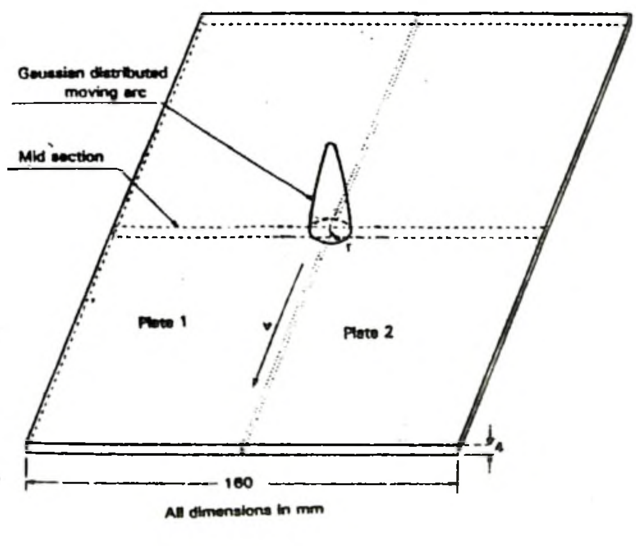

Fig 4 : Arc welding of steel plate

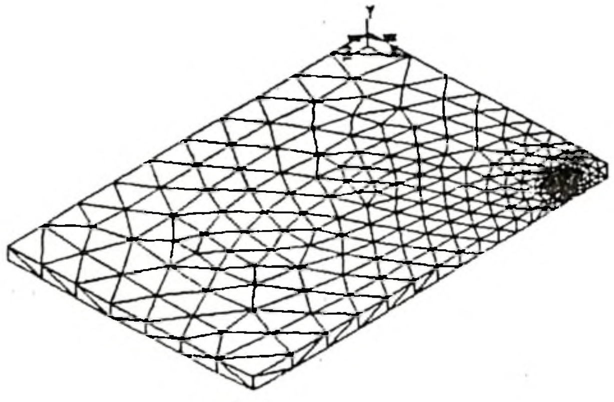

Fig 5 : Type of mesh for 120 mm x 80 mm x 4 mm plate after 3.603 second

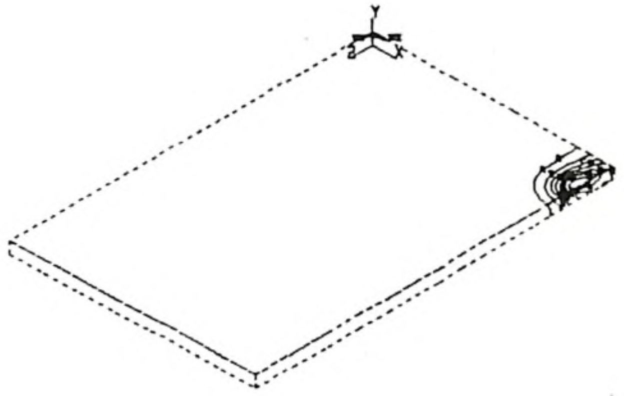

Temperature in ^{o}C
A = 225, B = 450, C = 675, D = 900,
E = 1125, F = 1350, G = 1575, H = 1800
Fig 6 : Temperature distribution at 3.603 second

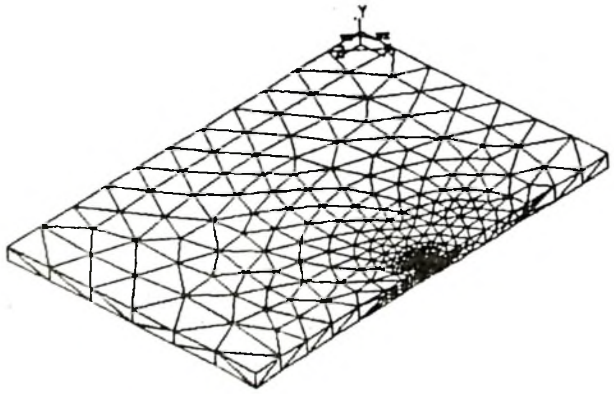

Fig 7 : Type of mesh for 120 mm x 80 mm x 4 mm plate after 18.018 second

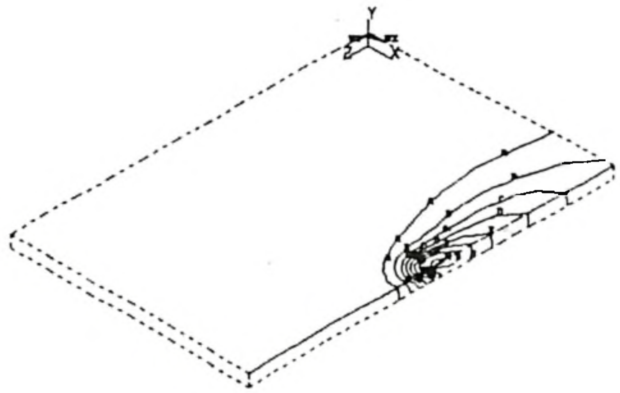

Temperature in ^{o}C
A = 225, B = 450, C = 675, D = 900,
E = 1125, F = 1350, G = 1575, H = 1800
Fig 8 : Temperature distribution at 18.018 s (mid section)

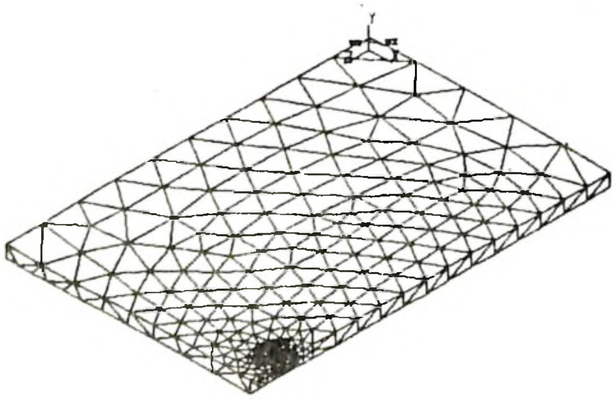

Fig 9 : Type of mesh for 120 mm x 80 mm x 4 mm plate after 32.432 second

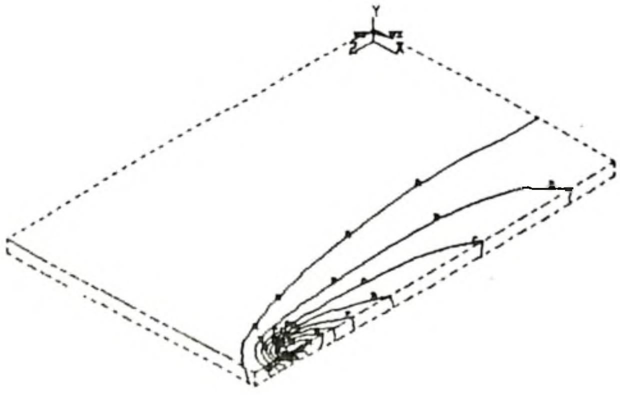

Temperature in ^{o}C
A = 225, B = 450, C = 675, D = 900,
E = 1125, F = 1350, G = 1575, H = 1800
Fig 10 : Temperature distribution at 32.432 second

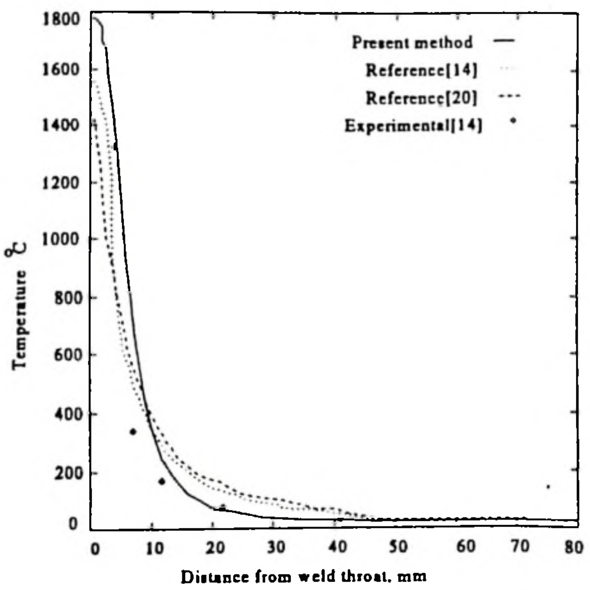

Fig 11 : Transverse temperature distribution at mid section during passing arc

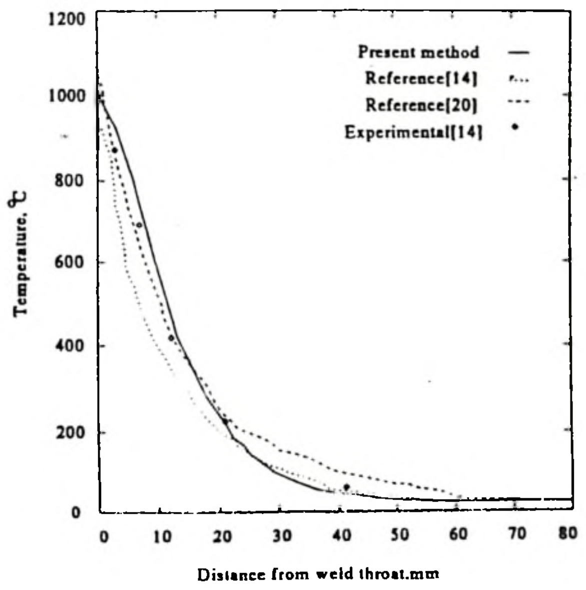

Fig 12 : Transverse temperature distribution at mid section 7.5 s after passing arc

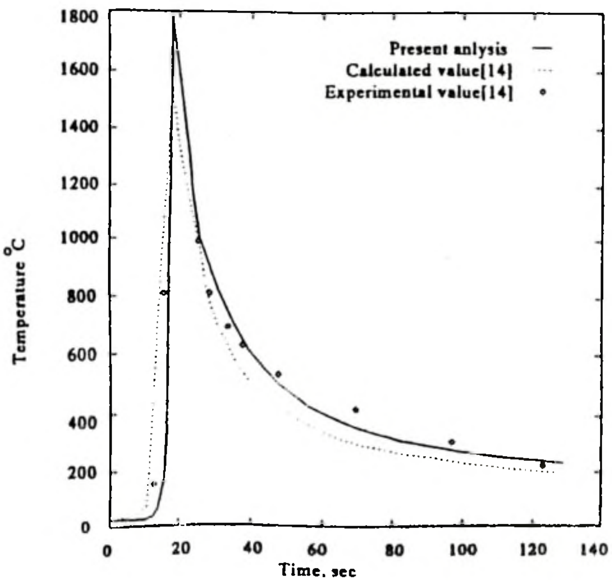

Fig 13 : Transverse history at weld throat at a distance 60 mm from the starting

Results

Figs. 6, 8 and 10 present the three dimensional temperature distributions at different positions of the welding arc. Temperature distribution at mid section at the time of passing arc (Fig. 11) and 7.5 s after passing arc (Fig. 12) have been compared with the experimental as well as the calculated values published in the literature. From the figures it can be concluded that results obtained by the present method are comparable. Fig. 13 shows that variation of temperature at any point predicted by present method approaches more closer to the experimental values. Most of the earlier models reported in the literature are two dimensional. Here, authors have successfully presented a three dimensional solution of heat flow in arc welding.

CONCLUSION

A 3-D heat flow in arc welding was analysed using FEM. Theoretically predicted values match closely with the experimental results published in the literature.

REFERENCES

1. *Rosenthal, D.*, Mathematical theory of heat distribution during welding and cutting, Welding Journal, May 1941, V 20, N 5, P 220s-234s.
2. *Rosenthal, D.*, The theory of moving sources of heat and its application to metal treatments, Transaction of the ASME, November 1946, V 68, P 849-866.
3. *Pavelic, V., Tanbakuchi, R., Uyehara, O.A. and Myera, P.S.*, Experimental and computed temperature histories in gas tungsten arc welding of thin plates, Welding Journal, July 1969, V 48, N 7, P 295s-305s.
4. *Graville, B.A.*, Weld cooling rates and heat-affected zone hardness in a carbon steel, Welding Journal, September 1973, V 52, N 9, P 377s-385s.
5. *Longworth, D.*, A numerical method to determine the temperature distribution around a moving weld pool. Moving boundary problems in heat flow and diffusion, Edited by J R Ockendon and W R Hodgkins, Clarendon press, Oxford ©1975, P 54-61.
6. *L J Segerlind*, "Applied finite element analysis", John Willy and Sons, Inc ©1976.
7. *G W Krutz and L J Segerlind*, "Finite element analysis of welded structures", Welding Journal, V 57, N 7, P 211s, July 1978.
8. *Andersson, B.A.B.*, Thermal stresses in submerged arc welded joint considering phase transformations, Transaction of the ASME, Journal of engineering materials and technology, October 1978, V 100, P 356-362.
9. *K Morgan, R W Lewis and O C Zienkiewicz*, "An improved algorithm for heat conduction problems with phase change", International Journal for numerical methods in engineering, V 12, Issue No 7, P 1191, 1978.
10. *Sharir, Y., Grill, A. and Pelleg, J.*, Computation of temperatures in thin tantalum sheet welding, Metallurgical Transactions B, June 1980, VIIB, N2, P 257-265.
11. *Kon, Sindo*, Simulation of heat flow during welding of thin plates, Metallurgical Transactions A, December 1981, V 12A, N 12, P 2025-2030.
12. *Papazoglou, V.J. and Masubuchi, K.*, Numerical analysis of thermal stresses during welding including phase transformation effects, Transactions of the ASME, Journal of pressure vessel technology, August 1982, V 104, P 198-203.
13. *John Goldak, Aditya Chakravarti, and Malcom Bibby*, "A new finite element model for welding heat sources", Metallurgical Transactions B, V 15B, N 2, P 299, June 1984.
14. *Argyris, J. H., Szimmat, J. and Willam, K.J.*, Finite element analysis of arc welding processes, Numerical methods in heat transfer, Volume iii, Edited by R W Lewis and K Morgan, John Wiley and Sons Ltd, ©1985, P 1-34.
15. *Kannatey-Asiby, Elijah Jr., Kikuchi, Noburu and Jallad, Abdel-Rahim*, Experimental finite element analysis of temperature distribution during arc welding, Transaction of the ASME, Journal of engineering materials and technology, January 1989, V III, N 1, P 9-18.
16. *Smith, N. J., McGrath, J.T., Gianetto, J.A. and Orr, R.F.*, Microstructure/Mechanical property relationships of submerged arc welds in HSLA 80 steel, Welding Journal, March 1989, V 68, N 3, P 112s-120s.
17. *Oldland, P.T., Ramsay, C.W., Matlock, D.K. and Olson, D.L.*, Significant features of high strength steel weld metal micro-structures, Welding Journal, April 1989, V 68, N 4, P 158s-168s.
18. *Joarder, A., Saha, S.C. and Ghose, A.K.*, Study of submerged arc weld metal and heat affected zone microstructures of plain carbon steel, Welding Journal, June 1991, V 70, N 6, P 141s-146s.
19. *Parkitny, R., Pawlak, A. and Piekarska, W.*, Thermal model of submerged arc welding, Material science and technology, September 1992, V 8, P 841-843.
20. *Prasad, N. Silva and Sankaranarayana, T.K.*, Finite element analysis of temperature distribution during arc welding using adaptive grid technique, Welding Journal, April 1996, V 75, N 4, P 123s-128s.

Acknowledgement

Received the Quarterly News Letter of The Indian Institute of Welding, Mumbai Branch
Numbers 1 & 2, Volume 3, January - June 1999.